Creep fatigue crack growth and fracture mechanisms of T/P91 power plant steel

F. Bassi, S. Foletti and A. Lo Conte*

List of symbols

a	Crack length/mm
a_0	Initial crack length/mm
C	Coefficient of the mean fit of da/dt vs C*, as obtained from CCG tests
C^*	Fracture mechanics parameter/MPa m h^{-1}
D	Coefficient of the Paris law as obtained from high temperature FCG tests
f	Frequency/Hz
F	Force/N
K	Stress intensity factor/MPa m$^{0\cdot5}$
m	Coefficient of the Paris law as obtained from HTF tests
N	Number of cycles
R	Load ratio
q	Coefficient of the mean fit of da/dt vs C*, as obtained from CCG tests
t	Time/h
T	Temperature/°C
W	Nominal size of the CT specimen/mm
σ_{ref}	Reference stress/MPa
$\dot{\varepsilon}_{ref}$	Secondary creep strain rate at the reference stress (1/h)

Introduction

The worldwide demands of power generation industries such as process cost reductions, high efficiency and flexibility in operating and maintaining the plants lead to the necessity of reliable remaining life assessment at elevated temperatures for engineering components. In particular, the continuous trend of higher operating temperatures, combined with the life extension of existing power plants, requires consistent experimental investigation as well as analytical approaches able to predict material behaviour under operating conditions.

Considering either design codes, which generally consider defect free structures,[1] and assessment codes[2–5] which address flaws and their treatment, European and International programs have been undertaken in cooperation with several power generation companies. A detailed description of these collaborative programs, their objectives and findings can be found in Ref. 6, where the historical and current technical concepts are reported.

As far as the criteria for structural assessment in presence of defects are concerned, the condition of high temperature failure strongly calls for reliable data for the design and in-service assessment.

In particular, loading situations related to high temperature and cyclic loads due to rapid load changes or fast run-up must be taken into account in the design of such engineering components. Standard procedures[1] can be applied when damage for creep and fatigue occur separately during plant operation. On the contrary, when fatigue and creep damage interact each other, the unexpected onset of cracking and consequently reduced component endurance can occur. Furthermore, in complex situations when startups lead to rapid increase on key operating parameters, such as temperature, pressures and mass flow, high thermal stresses can be generated, mainly due to uneven temperature distribution. This can cause an increased level of components stress, which has often a detrimental effect on material degradation and components life.

Under this difficult scenario, the understanding of materials response to thermal–mechanical stresses, creep crack growth, creep-fatigue damage mechanics and their

Politecnico di Milano, Department of Mechanical Engineering, Via La Masa 1, 20156, Milan, Italy

*Corresponding author, email antonietta.loconte@polimi.it

mutual interactions becomes extremely important for the development and application of reliable assessment models.

To address these items, the present paper deals with the understanding and prediction of crack initiation and growth in the creep fatigue regime of P/T91 grade steel. Considerable work in the past was focused on creep-fatigue crack formation,[7,8] on test conditions finalised to provide data that can be used such as material properties for crack growth prediction in power plant components,[9,10] and on phenomenological and physical approaches to describe the effect of fatigue crack interaction.[11,12]

The aim of the research described in this paper is to report the results of a dedicated experimental program to collect homogeneous experimental data of creep crack growth (CCG), high temperature fatigue (HTF), and creep fatigue crack growth (CFCG) in order to gain information about how the crack behaviour of this material, at the ongoing temperature of 600°C, is affected by the creep fatigue interaction effect.

Microscopic features of the creep fatigue damage were observed along the crack path, on polished and etched cross sections of the tested specimens. The dominant damage mechanism is the formation of microvoids and microcracks associated with the crack tip, due to creep deformation during the hold time.

In order to predict the experimentally measured crack growth rate, a simple summation rule is used. The application of the superposition model for the total crack growth rate calculation is based on the creep crack growth rate and on high temperature fatigue crack growth rate, experimentally obtained on the same batch of material used for creep fatigue crack growth tests. The model well describes the observed behaviour under creep fatigue loading.

Experimental methods

Material and specimen preparation

The tested material is a modified 9Cr-1Mo martensitic steel (T/P91) widely used in pipes and boilers of power generation plants. Table 1 summarises tensile and creep properties at room temperature and at the temperature of 600°C chosen for the present investigation.[13] Creep properties were determined with dedicated tests, and two different set of coefficients for Norton's equation were obtained at low and high stress levels.

The specimen geometry used for the experimental program was the standard ½ inch Compact Tension C(T) specimen. The specimens were fatigue pre-cracked to an initial crack length to width ratio (a/W) of 0·47–0·48, under the condition of a load ratio $R=0{\cdot}1$ at room temperature. Subsequently side grooves, each one 10% of the thickness deep, were machined on the plane of the crack propagation.

The specimens intended to be tested with potential drop measurements of the crack propagation were also equipped with an appropriate scheme of electrical leads.

Experimental program and procedure

In order to conduct the experimental program, both electrically actuated lever arm creep and servo-hydraulic test machines were used. The set-up of the electrically actuated lever arm creep machine included: a convection furnace with three controlled zones, ensuring the required temperature stability during the test, a DC potential drop system to monitor the crack initiation and propagation,[14] and a load line extensometer to measure the load line displacement for experimental calculation of the C* fracture mechanics parameter (Fig. 1*a*). The set-up of the servo-hydraulic test machines included: a two zones convection furnace for the control of the temperature during the test, and a high temperature extensometer of type 'EPSILON 3548COD' for monitoring crack extension on the basis of the compliance method (Fig. 1*b*).

The matrix of the experimental program and of the test parameters is reported in Table 2. Creep crack growth (CCG) tests were all performed with the electrically actuated lever arm machine, with different values of initial stress intensity factor, according to ASTM E1457.[15] High temperature FCG tests were all performed with the servo-hydraulic machine, at the initial magnitude of the stress intensity factor of 17 MPa $m^{1/2}$, with load ratios of $R=0{\cdot}1$, and 0·7 and with loading frequencies of 1 and 10 Hz. The procedure was in accordance with ASTM E647-13.[16] Creep Fatigue Crack Growth (CFCG) tests were performed according to ASTM 2760-10.[17] with the cyclic loading shown in Fig. 2. For all tests the maximum magnitude of the stress intensity factor was of 23 MPa $m^{1/2}$ and, the load ratio R equal to 0·1, while the hold times were 0·1, 1, and 10 h. As reported in Table 2, the condition '0·1 h of hold time' was tested both using the electrically actuated lever arm machine, with DCPD monitoring of the crack length, and using the servo-hydraulic machine, with compliance measurement of the crack length. All the experimental tests were carried out at 600 ± 1°C.

An example of a crack length versus time curve is reported in Fig. 3 for the CCG test with a value of $K_{initial}$ equal to 18 MPa $m^{1/2}$. Fitting curve, crack length versus time, of all the tests gave the time (t_i) corresponding to the technical crack growth initiation $\Delta a=0{\cdot}2$ mm, and the corresponding crack growth rate expressed as da/dt or da/dN. At the end of the tests, specimens were broken in liquid nitrogen. Half specimens were used for observations of fracture surface and measurement of the initial and final crack length, according to the scheme shown in the detail of Fig. 3. The other specimen halves were sectioned for SEM observations of the damage along the path of crack propagation.

Table 1 T/P91 grade mechanical and creep properties at room/on going temperature

Property		24°C	600°C
Young's modulus/GPa		200	167
Yield strength/MPa		532	465
Ultimate strength/MPa		708	517
Low stresses (<120 MPa)	Constant/$(MPa)^{-n}$ h^{-1}	…	$2{\cdot}7 \times 10^{-14}$
Norton parameters	Exponent	…	4
High stresses (>120 MPa)	Constant/$(MPa)^{-n}$ h^{-1}	…	$2{\cdot}2 \times 10^{-39}$
Norton parameters	Exponent	…	16
10^5 h creep strength/MPa		…	90

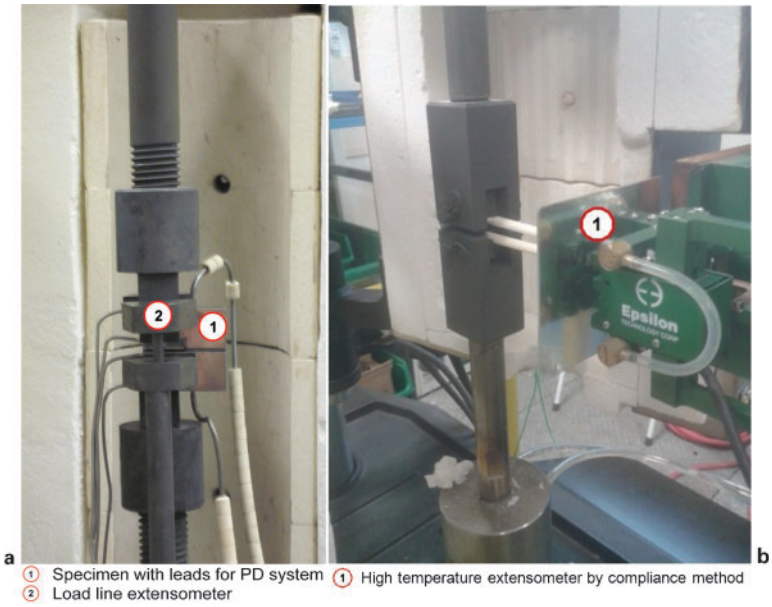

1 Experimental set-up: *a* electrically actuated lever arm machine with PD measurements of crack growth and *b* servo-hydraulic machine with high temperature extensometer for measurements of crack growth by compliance method

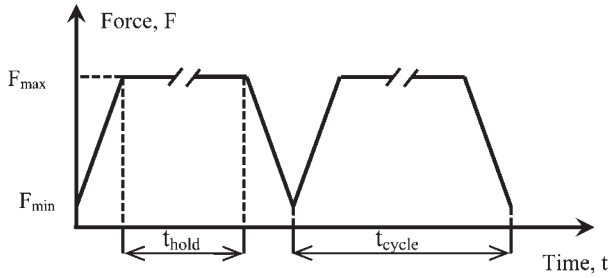

2 Cyclic loading for CFCG tests

Results and discussion

Crack propagation

The creep fatigue curves for the different examined hold times are reported in Fig. 4. In this graph, and in the following, a normalisation has been applied in order to fit data in the range up to unity. All the tests have been performed at the same nominal range of the stress intensity factor ($K_{initial,\ MAX}$=23 MPa m$^{1/2}$, R=0·1). A comparison with the creep crack growth test at comparable nominal stress intensity factor (K_{max}=22 MPa m$^{1/2}$) is also reported in the same figure. The diagram shows that creep fatigue loading conditions, with hold times of 1 h and 10 h, lead to curves matching well the curve obtained applying creep loading, without fatigue interaction; while

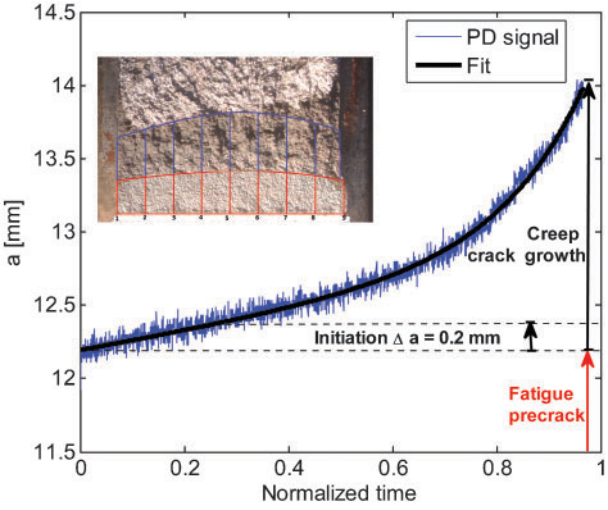

3 Crack length versus time curve for CCG test with $K_{initial}$ equal to 18 MPa m$^{1/2}$ and detail of fracture surface

in creep fatigue loading, with hold time of 0·1 h, the crack behaviour shows a strong effect of the cyclic loading. Crack propagation during creep-fatigue tests is described in terms of the fracture mechanics parameter C^*. Figure 5 shows the results of crack propagation rate versus C^* parameter for the creep-fatigue tests compared with results

Table 2 Experimental program and test parameters

Test type	Set-up	T/°C	a_0/W	R (F_{min}/F_{max})	$K_{initial,\ MAX}$/MPa m$^{1/2}$	f/Hz	t_{hold}/h
CCG	Electrically actuated	600	0·45–0·5	…	15	…	…
				…	20	…	…
				…	22	…	…
				…	28	…	…
FCG	Servo-hydraulic	600	0·3–0·35	0·1	17	1	…
				0·1		10	…
				0·7		1	…
				0·7		10	…
CFCG	Electrically actuated	600	0·48	0·1	23	…	0·1
	Servo-hydraulic		0·31			…	0·1
	Electrically actuated		0·5			…	1
	Electrically actuated		0·48			…	10

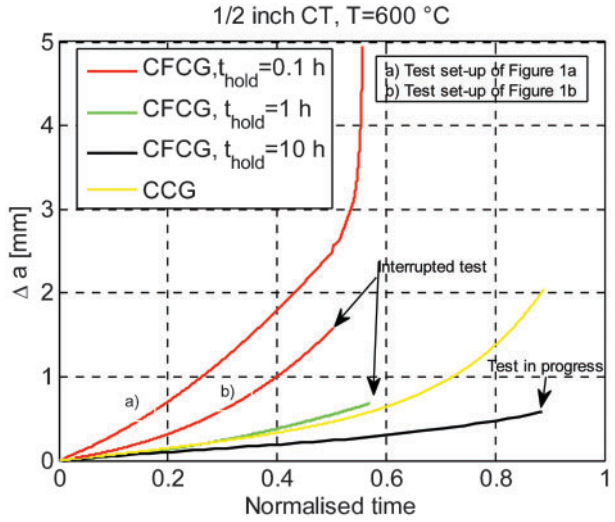

4 **Crack propagation versus normalised time for CFCG tests at $K_{initial,MAX}$=23 MPa m$^{0·5}$, R=0·1, and for CCG test at K=22 MPam$^{0·5}$**

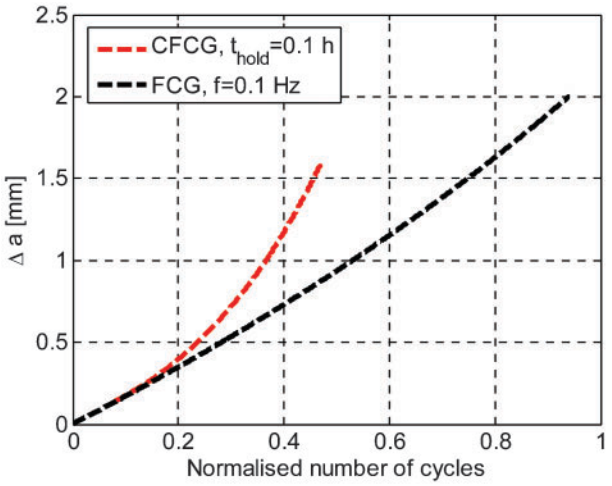

6 **Crack propagation versus normalised number of cycles for CFCG tests with hold time equal to 0·1 h and for FCG tests at f=1 Hz: for both tests K_{MAX}= 23 MPa m$^{1/2}$, R=0·1**

of creep crack growth tests. The cyclic loading seems to have only an influence in the initial phase of the test. The interaction of cycling loading with the blunting of crack tip results in a reduction of the C^* parameter and of the related creep crack growth rate at which crack growth starts, and in a less evident nose shape of the crack propagation rate versus C^* parameter. This effect was observed for all the investigated values of hold time. On the other hand, the relationship between crack growth rate and C^* for creep fatigue is well fitted by the average curve and the scatter band of the creep crack growth rate.

The results of creep fatigue tests are also compared with results of high temperature fatigue tests. Figure 6 shows the creep fatigue curve, R=0·1, and hold time of 0·1 h, compared with the pure fatigue curve obtained with the same load cycle and f=1 Hz; Fig. 7 reports the Paris diagram for the material. It is evident that the creep fatigue behaviour cannot be described by the Paris law. With increasing hold time, time dependent effects became important and an increase in the cyclic growth rate is observed with respect to the prediction of the Paris law.

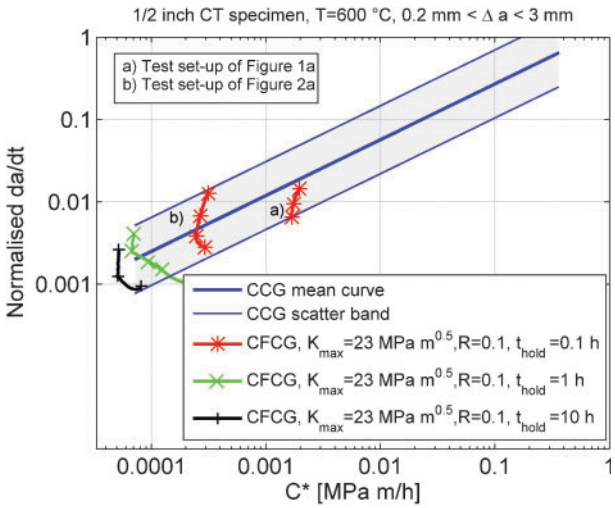

5 **Crack propagation rate versus C^* parameter: CFCG tests and CCG tests**

Crack growth mechanism

Microscopic features of the creep fatigue damage were observed along the crack path, on polished and etched cross sections of the tested specimens. As shown in Fig. 8 for creep fatigue tests with 0·1 h of hold time, the creep fatigue crack front is highly bifurcated (detail A and B), and the cracks appear widely opened and filled with oxide (detail C). The dominant damage mechanism is the formation of microvoids and microcracks (detail D), due to creep deformation during the hold time. Under cyclic loading, the creep damage along the crack path accounts for a creep fatigue crack propagation at lower level C^* values, with respect to the creep crack growth at the same initial stress intensity factor, as observed in Fig. 5. At the same time creep damage along the crack path also accounts for an increase of the crack growth rate with increasing hold time and stress intensity factor as observed in Fig. 7.

Creep-fatigue superposition model

The description of creep fatigue crack growth as a simple linear summation rule, on the basis of pure creep and high temperature fatigue contents has been successfully proposed.[17,18] For creep ductile materials the following equation was proposed

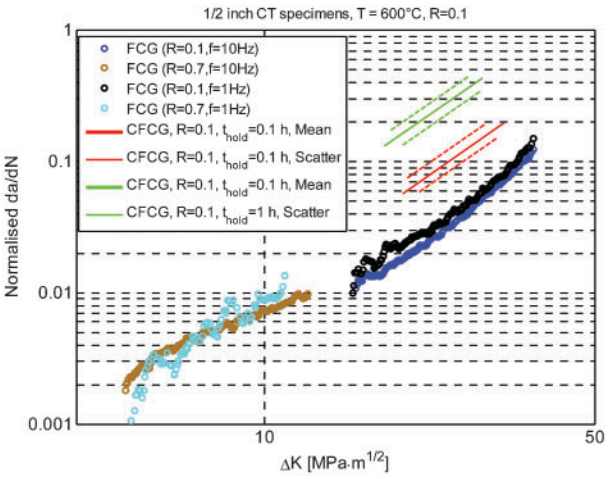

7 **Normalised crack propagation rate versus ΔK: experimental range for CFCG tests and results of FCG tests**

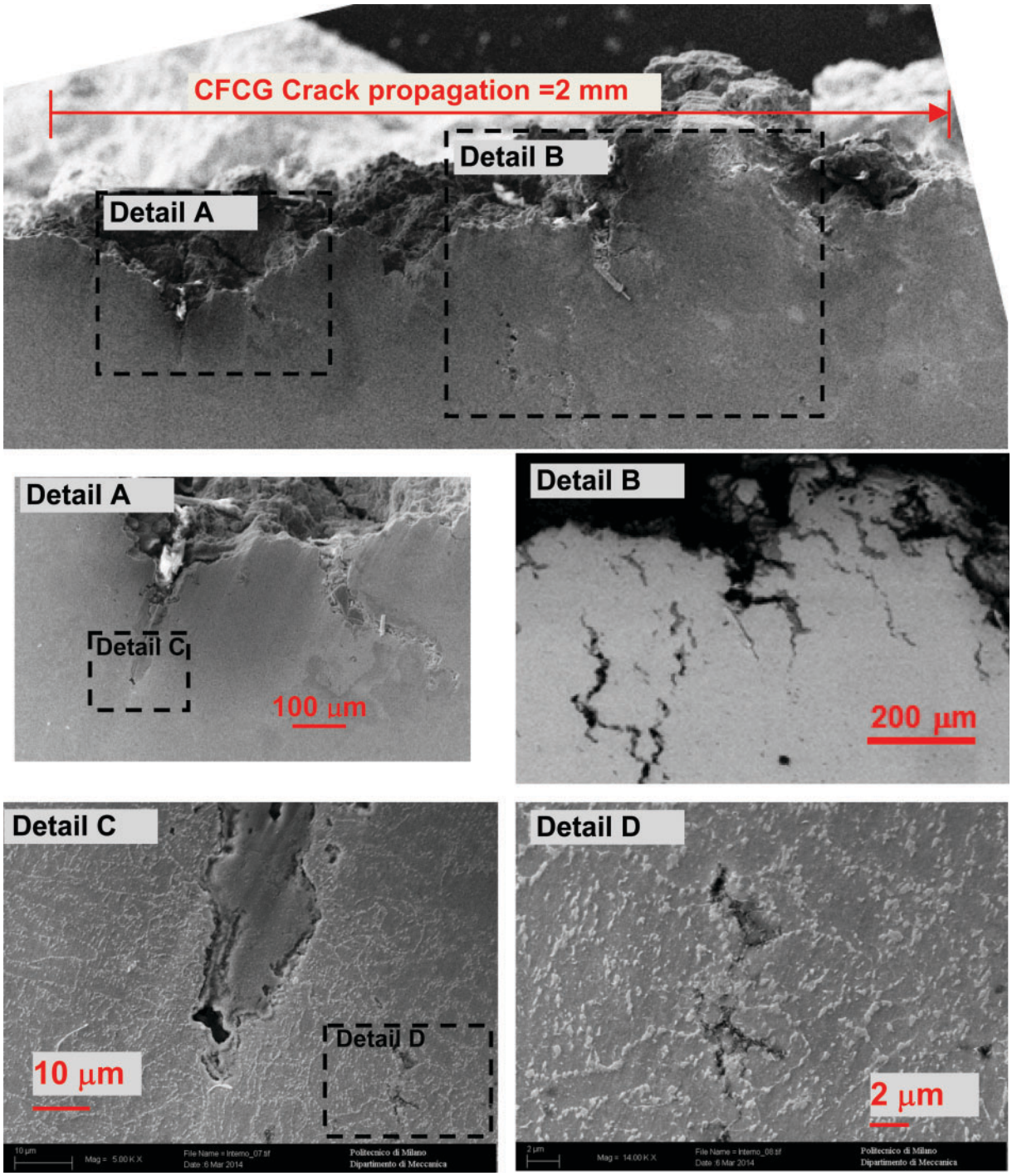

8 SEM observations of creep fatigue damage along crack front for creep fatigue tests with 0·1 hold time; top: crack front from tip of fatigue precrack, on left, to end of creep fatigue propagation, on right; detail A: bifurcation of crack at start of creep fatigue propagation; detail B: back scattering image of creep damage along crack front; detail C: after etching cracks appear widely opened and filled with oxide; detail D Voids and microcracks characterise creep fatigue damage

$$\frac{da}{dN} = C\Delta K^{m} + t_{hold} D (C^{*})^{q} \quad (1)$$

The first term is the pure fatigue contribution, where C and m are the coefficients of the Paris law as obtained from HTF tests (Fig. 7). The second term is the creep contribution, where t_{hold} is the hold time, D and q are the coefficients of the mean fit of da/dt versus C^*, as obtained from high temperature FCG tests (Fig. 5).

Figure 9 shows the prediction of the crack growth rate for creep fatigue tests at different hold times according to equation (1).

The initial value of the maximum stress intensity factor has been fixed at 23 MPa $m^{0·5}$, with a ratio R=0·1, while the C^* parameter has been evaluated as

$$C^{*} = \sigma_{ref} \dot{\varepsilon}_{ref} \left(\frac{K}{\sigma_{ref}} \right)^{2} \quad (2)$$

where σ_{ref} is the reference stress for the CT specimen[5] and $\dot{\varepsilon}_{ref}$ is the secondary creep strain rate obtained on the basis of the Norton law of the material (see Table 1).

The experimental creep fatigue crack propagation for each test is the value of crack propagation immediately after crack initiation.

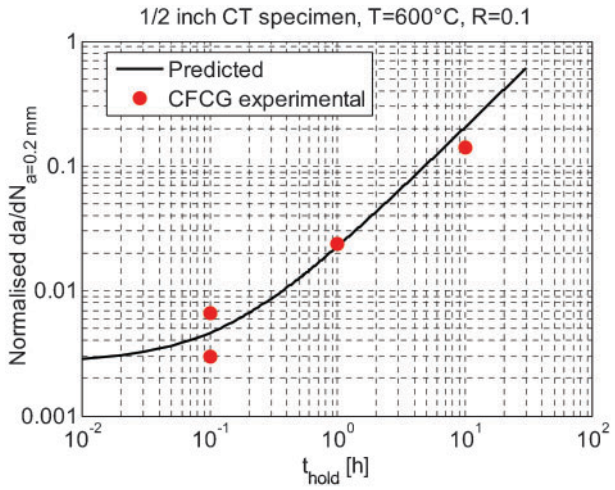

9 Normalised creep-fatigue crack growth rate versus holding time: CFCG tests with initial value of maximum stress intensity factor is 23 MPa $m^{0.5}$, and R=0·1

The comparison between the experimentally determined values and the predicted ones shows that the simple superposition of high temperature fatigue crack growth and creep crack growth well describes the behaviour under creep fatigue loading. It is worth noting that, both the HTF tests and the CCG tests were performed on the same batch of material used for the creep fatigue tests. Moreover, the trend of Fig. 9 suggests that the investigated values of holding time fall in the pure HTF regime (0·1 h) or in the pure CCG regime (1 and 10 h). For holding time between 0·1 and 1 h a cycle/time dependent transition can be expected.

In this range an interaction term in the equation (1) should be required in order to match the creep fatigue growth rate. According to the operation cycle of components, for which the investigated material is used, experimental tests can be planned to investigate this range of holding time and to evaluate this hypothesis.

Conclusions

In this paper creep fatigue crack growth tests for P91 material, conducted at 600°C on standard C(T) specimens with 0·1, 1 and 10 h hold times, have been presented.

The interaction of cyclic loading with the crack tip blunting resulted in a reduction of the C^* parameter and the related creep crack growth at which the crack growth starts, but the relationship between crack growth rate and C^* parameter obtained on the basis of CCG tests is still valid for creep fatigue crack growth rate.

From the SEM analysis of polished and etched cross-sections along the crack paths of the tested specimens, it is revealed that the dominant damage mechanism is the formation of microvoids and microcracks ahead of the crack tip, due to creep deformation during the hold time.

A simple superposition of fatigue crack growth rate and creep crack growth rate has been used to predict the experimentally measured crack growth rate. For the investigated values of hold time, the application of a superposition model based on CCG data and HTF data experimentally obtained on the same batch of material used for creep fatigue crack growth tests, well describes the behaviour under creep fatigue loading.

Acknowledgements

The work is part of the activities within a research project, headed by Prof. S. Beretta, between the Department of Mechanical Engineering at Politecnico di Milano and Tenaris Dalmine. Dr. Mario Rossi, director of Tenaris Dalmine Research and Development Center, is kindly acknowledged for the permission to publish this paper. The authors are especially grateful to Prof. Stefano Beretta from Politecnico di Milano and Dr Mihaela E. Cristea from Dalmine R&D, for their support during the development of the present work.

References

1. ASME Section III: 'Rules for construction of nuclear power plant components', Division 1, Subsection NH, Class 1 components in elevated temperature service, ASME, 1995.
2. British Standard BS7910: 'Guidance on methods for assessing the acceptability of flaws in metallic structures', British Standards Institution, 2000.
3. R5: 'An assessment procedure for the high temperature response of structures', (ed. I. W. Goodall), Issue 3; 2003, London, British Energy-UK.
4. A16: 'Guide for leak before break analysis and defect assessment', RCC-MR, Appendix A16, Edition 2002, AFCEN no. 94-2002.
5. M. Koçak, S. Webster, J. J. Janosch, R. A. Ainsworth and R. Koers: 'FITNET: Fitness-for-Service Procedure - Final Draft MK7', 2006.
6. K. Nikbin: 'Creep/fatigue crack growth testing, modelling and component life assessment of welds', Proc. 6th Int. Conf. on 'Creep, fatigue and creep-fatigue interaction [CF-6]', *Proced. Eng.*, 2013, 55, 380–393.
7. B. Fournier, M. Sauzay, C. Caes, M. Noblecourt, M. Mottot, A. Bougault, V. Rabeau, J. Man, O. Gillia, P. Lemoine and A. Pineau: 'Creep-fatigue-oxidation interactions in a 9Cr-1Mo martensitic steel. Part III: lifetime prediction', *Int. J. Fatigue*, 2008, **30**, 1797–1812.
8. M. Speicher, A. Klenk and K. Coleman: 'Creep-fatigue interaction in P91 steel', Proc. 13th Conf. on 'Fracture', Beijing, China, June 2013. The Chinese Society of Theoretical and Applied Mechanics, S22–018.
9. S. B. Narasimhachary and A. Saxena: 'Crack growth behavior of 9Cr-1Mo(P91) steel under creep-fatigue conditions', *Int. J. Fatigue*, 2013, **56**, 106–113.
10. J. Granacher, A. Klenk, M. Tramer, G. Schellenberg, F. Mueller and J. Ewald: 'Creep fatigue crack behavior of two power plant steels', *Int. J. Press. Vessel Pip.*, 2001, **78**, 909–920.
11. G. Zhang, Y. Zhao F. Xue, Z. Wang, J. Mei, L. Zhang and C. Zhou: 'Study of life prediction and damage mechanism for modified 9Cr-1Mo steel under creep-fatigue interaction', *J. Press. Vessel Technol.*, 2013, **135**, 0414103.
12. M. Tabuchi, J. Ha, H. Hongo, T. Watanabe and T. Yokobori, Jr: 'Experimental and numerical study on the relationship between creep crack growth properties and fracture mechanism', *Metall. Mater. Trans. A*, 2004, **35A**, 1757–1764.
13. A. Lo Conte, M. E. Cristea, C. Turconi and R. Sanfilippo: 'Structural integrity assessment of pipes for high temperature applications', Proc. of the ECCC- Creep & Fracture Conf., May 2014, Rome, Italy. Centro Svilluppo Materiali, 2.
14. G. Belloni, E. Gariboldi, A. Lo Conte, M. Tono and P. Speranzoso: 'On the experimental calibration of potential drop system for crack length of compact tension specimen measurements', *J. Test. Evaluat.*, 2002, **30**, 461–469
15. ASTM: 'ASTM E 1457-07: standard test method for measurement of creep crack growth rates in metals', 2007.
16. ASTM: 'ASTM E647-13: standard test method for measurement of fatigue crack growth rates', 2013.
17. ASTM: 'ASTM E2760-10: standard test method for creep-fatigue crack growth testing', 2010.
18. F. D. Javanroodi and K. M. Nikbin: 'The fracture mechanics concept of creep and creep/fatigue crack growth in life assessment', *Int. J. Eng. Sci.*, 2006, **17**, (3–4), 1–7.